ISSN 1063-7842, Technical Physics, 2019, Vol. 64, No. 3, pp. 399–403. © Pleiades Publishing, Ltd., 2019.
Russian Text © A.A. Badarin, S.A. Kurkin, N.S. Frolov, A.O. Pak, A.E. Khramov, 2019, published in Zhurnal Tekhnicheskoi Fiziki, 2019, Vol. 89, No. 3, pp. 436–440.

RADIOPHYSICS

Analysis and Optimization of the Characteristics of Superpower Virtode Generation

A. A. Badarin[a,b,*], S. A. Kurkin[a,b], N. S. Frolov[a,b], A. O. Pak[c], and A. E. Khramov[a,b]

[a] *Chernyshevskii Saratov National Research State University, Saratov, 410012 Russia*
[b] *Gagarin Saratov State Technical University, Saratov, 410054 Russia*
[c] *Belarusian State University of Informatics and Radioelectronics, Minsk, 220013 Belarus*
**e-mail: Badarin.a.a.@mail.ru*

Received March 15, 2018; in final form, October 2, 2018

Abstract—We report on the results of the 3D numerical simulation of perspective design of an oscillator based on an external-feedback virtual cathode (virtode), as well as optimization of characteristics of its generation. We have analyzed the effect of beam parameters on the virtode output characteristics. In particular, we have obtained the dependence of the efficiency on the feeding voltage and on the current being injected. We have studied the effect of beam velocity premodulation and electron velocity spread on virtode generation characteristics. It has been established that the introduction of premodulation sharply increases the generation efficiency up to 13% for optimal parameters. The possibility of stable generation in the virtode at relatively large spread in electron velocities has been demonstrated.

DOI: 10.1134/S1063784219030034

INTRODUCTION

The study of systems with relativistic electron beams (REBs) is an important and topical problem in contemporary plasma physics and high-power microwave electronics in view of the important role of REBs in the following fields of application: plasma heating, generation of superpower microwave radiation, ion acceleration, etc. [1, 2]. Many processes occurring in REBs (e.g., evolution of various types of beam–plasma instabilities) have been studied insufficiently. The study and optimization of relativistic oscillators operating in virtual cathodes, which have attracted attention of researchers since the end of the 1970s, are among the main trends in investigations in high-power vacuum and plasma electronics [1, 3–16]. Devices based on virtual cathodes (such as vircator, readitron, and virtode) form a special class of microwave oscillators and bremsstrahlung amplifiers with operation based on the formation of a virtual cathode (VC) in a (usually relativistic) electron beam with supercritical current [1, 3, 5, 17–20]. The interest in such oscillators is due to their advantages including a very high output microwave radiation power, the simplicity of design (in particular, vircators can operate without an external focusing magnetic field), fast generation start, the possibility of simple frequency tuning and switching of regimes, and low requirements to the electron beam quality [1, 6, 8, 21, 22]. The latter property is important in the injection of a short-pulse and low-Q beam formed by an explosive-emission electron gun into the system [23].

Nevertheless, oscillators based on a virtual cathode have some serious drawbacks such as the instability of generation frequency (for certain designs) and a low efficiency, which limit their wide application [1]. The introduction of additional electromagnetic feedback in such oscillators suppresses the above-mentioned undesirable effects [24–26]. The double-gap virtode, which was studied, in particular, in [25–27], is a promising modification of VC-based oscillators with electromagnetic feedback.

At present, there are some important questions in investigations of virtodes, which require further research. In particular, the effect of electron beam Q factor and its remodulation on virtode generation characteristics has not been investigated, and optimization of the device for attaining maximal generation efficiency has not been performed. In this respect, this study is a continuation of investigations of double-gap virtodes and is devoted to analysis of the above-mentioned problems.

1. MODEL

We analyzed virtode generation characteristics using the particle-in-cell (PIC) method realized in three spatial coordinates [28], which proved to be quite effective. This method is based on self-consistent numerical solution of the Maxwell equations by the

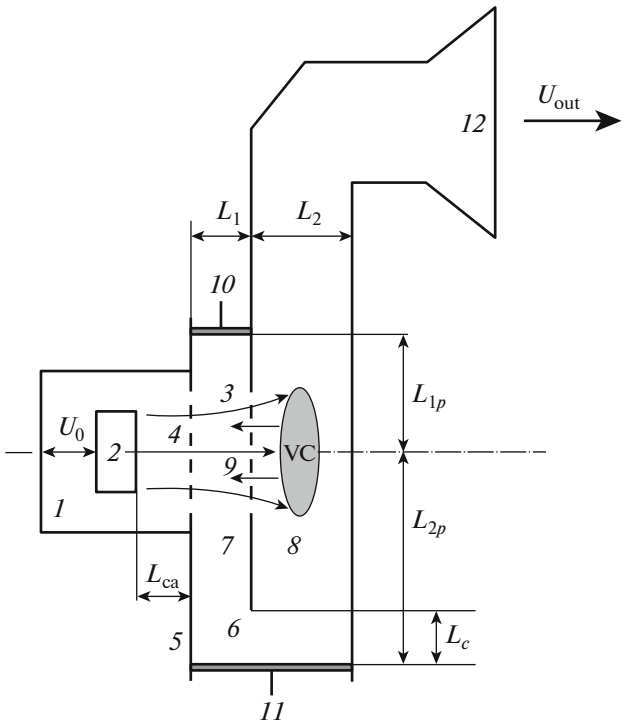

Fig. 1. Schematic diagram of a virtode: (*1*) electron gun; (*2*) cathode; (*3*) continuous relativistic electron beam; (*4*) anode grid; (*5*) double-gap cavity; (*6*) coupling window; (*7*) first gap in the double-gap cavity; (*8*) second gap; (*9*) grid in the wall between the gaps; (*10*) plunger controlling the first gap height (*11*) plunger controlling the coupling window width; (*12*) power output; U_0 is the accelerating voltage; L_{ca} is the cathode–anode distance; L_1 and L_2 are the lengths of the first and second section, respectively; L_{1p} and L_{2p} are the positions of the first and second plungers, respectively; L_c is the length of the coupling window; U_{out} is the output signal; and VC is the schematic of the virtual cathode region.

finite-difference in the time domain (FDTD) method and relativistic equations of motion, which describe the behavior of particles. The FDTD method is based on discretization of the Maxwell equations written in differential form in the Cartesian system of coordinates. In this case, the grids for the E and H fields are shifted relative to each other by half the sampling interval in time and in each spatial coordinate. Such a grid is known as the Yi grid. The finite-difference Maxwell equations make it possible to determine fields E and H on a preset time interval from the known values of the fields in the previous step.

Thus, we first calculate the electromagnetic fields in accordance with the Maxwell equations and then solve the equations of motion for each coarse particle. The time and space intervals are chosen in accordance with the Courant–Friedrichs–Lewy condition [28]. In turn, the motion of a particle determines the current density required for calculating the electromagnetic fields in accordance with the Maxwell equations on the next time step. In this way, the law of current and charge conservation is ensured. In aggregate, such an approach ensures a high degree of reliability and accuracy of the results.

Let us now consider the scheme of the virtode under investigation (Fig. 1) [25]. The model contains the following main structural elements: electron gun *1* in the form of a cylindrical vacuum diode with explosive emission cathode *2*, which produces a high-intensity continuous electron beam *3* with a current density on the order of 10^6–10^7 A/cm^2; anode grid *4*, double-gap cavity *5* with coupling window *6* between the gaps, grid (usually foil) *9* in the wall between the gaps, and power output *12* in the form of a waveguide with a horn antenna connected to the second gap in the cavity, as well as plungers *10* and *11*, which make it possible to control the coupling window width and the modulation cavity parameters. This device is intended for generating high-intensity microwave radiation pulses and has the following operating principle. A continuous cylindrical relativistic electron beam with a current exceeding the second critical current is formed in the cylindrical vacuum diode with explosive emission cathode without an external focusing magnetic field and is then transported through the anode grid to the double-gap cavity in the direction perpendicular to its larger wall. The cavity gaps are sections of electrodynamically coupled rectangular waveguides. The electron beam gets from first gap *7* to second gap *8* after flying through a metal foil, which is located at the wall separating the gaps. In fact, the first gap plays the role of a modulator ensuring the feedback effect, while the second gap is the interaction chamber intended for the formation and subsequent energy removal in the VC. During VC formation, one of the lower modes is excited in the second cavity gap, which is emitted into vacuum via the horn antenna connected through the waveguide to the upper boundary of the second gap. Additional electromagnetic feedback is formed by an electromagnetic wave penetrating through the feedback window from the second to the first gap of the cavity, which makes it possible to increase the efficiency and stability of the virtode emission frequency.

It should be noted that electromagnetic field oscillations in the second gap, which are produced by a nonstationary VC, excite field oscillations in the first gap, which leads to modulation of the transmitted electron beam at the VC oscillation frequency. Therefore, the maintaining of the optimal phase shift between electromagnetic field oscillations on the beam axis in the first and second gaps is an important factor determining the geometry of the cavity. According to [29], an attempt was made to organize the regime of synphase fields ($\delta\phi = 0$) in the virtode, where $\delta\phi$ is the phase shift between the fields in the gaps. The positions of plungers *10* and *11* are chosen in such a way that their separation from the beam axis is about $3l/4$, where l is the wavelength of output signal oscillations. In this case, a standing wave consisting of

three half-waves and symmetric relative to the beam axis is formed in the first gap. As a result, the beam passes through antinodes of the field in the first and second gaps and effectively interacts with the electromagnetic field. Obviously, the frequency of oscillations of the output radiation is completely determined by the cavity size and can be varied by appropriate mechanical tuning of plungers *10* and *11* (see Fig. 1).

2. ANALYSIS OF GENERATION CHARACTERISTICS

We have performed multiparametric numerical optimization of the virtode geometry for increasing efficiency and generation frequency stability. The geometrical parameters determined for the system correspond to the conditions and requirements imposed on such devices. We have determined the following optimal geometrical parameters of the relativistic virtode: cathode radius r_c = 43 mm, electron gun radius r_g = 47.3 mm, distance between the cathode and anode grid L_{ca} = 24.4 mm, first gap length L_1 = 23.7 mm, distance between the upper piston in the first gap and beam axis L_{1p} = 166.5 mm, distance between the lower piston and beam axis L_{2p} = 174.4 mm, length of the second gap L_2 = 91.7 mm, position of the output waveguide relative to beam axis L_{out} = 272.4 mm, cavity width (which is the same in both gaps) D = 115.56 mm, and coupling window width L_c = 9.8 mm.

We have analyzed the effect of beam parameters on virtode generation characteristics. For this, we constructed the efficiency dependence on the feeding voltage level in the gun block (Fig. 2a). It can clearly be seen that the maximal virtode efficiency attains a value of about 4% for an accelerating voltage of 600 kV. Upon a further increase in the accelerating voltage, the generator efficiency decreases, demonstrating local maxima and minima. For high accelerating voltages $U_0 > 1.4$ MV, the efficiency turned out to be quite low (less than 0.5%). The optimal value of U_0 corresponds to the regime with the most stable generation frequency. Deviation of the accelerating voltage from the optimal value in any direction deteriorates the generation stability, an increase in U_0 leading to a delay in generation. Analogous investigations were performed with a variation of the REB current (Fig. 2b). The current dependence of efficiency turned out to be smoother with a single characteristic peak corresponding to a current of about 15 kA.

To analyze the effect of the noise spread of electrons, the beam was injected into the system with a preset spread in energy and in the electron injection angles in the system; in this case, a uniform distribution function was used. Therefore, the energies of injected electrons are distributed uniformly in the interval $[E_0 - \Delta E, E_0 + \Delta E]$ (where E_0 is the mean initial energy of the beam and ΔE is the energy spread parameter), while the angles of injection relative to the normal to the injection plane fall in the range $[-\Delta\alpha, \Delta\alpha]$ (where $\Delta\alpha$ is the angular spread parameter in degrees).

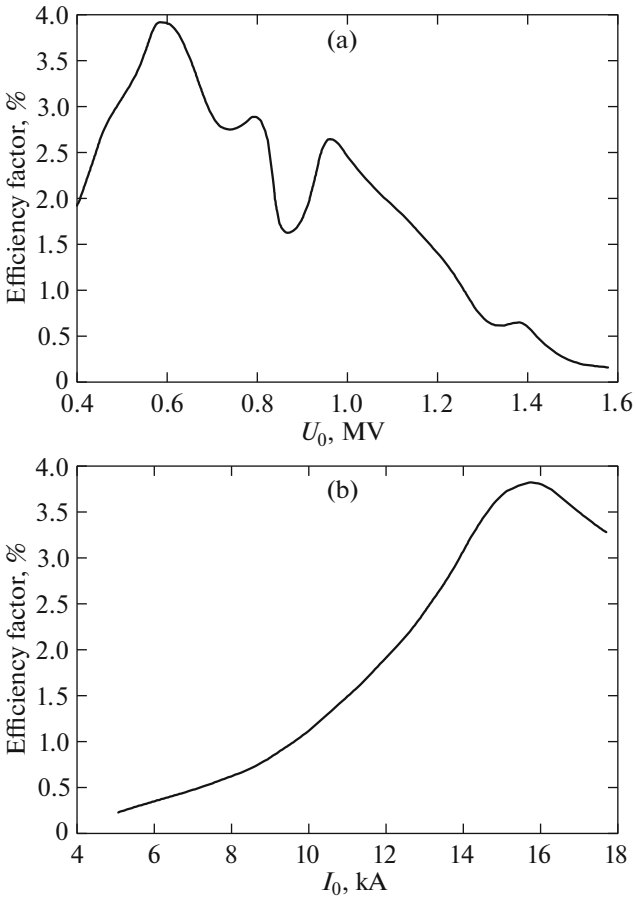

Fig. 2. Dependence of the virtode efficiency (a) on accelerating voltage and (b) on beam current.

It was found that an increase in the noise spread level of injected electrons leads to a decrease in the output power (Fig. 3); the electron injection angle spread produces a stronger effect (for example, for $\Delta\alpha > 18$ and $\Delta E = 0$, the output power almost vanishes, and failure of oscillation actually occurs). An increase in energy spread ΔE from 0 to 75% (at $\Delta\alpha = 0$) reduces the output voltage by 3–4 times. It was also revealed that the value of $\Delta\alpha$ at which failure of oscillations occurs decreases upon an increase in energy spread ΔE from 0 to 5%. Conversely, for $\Delta E > 5\%$, this quantity increases with ΔE (see Fig. 3). From the physical point of view, the failure of oscillations in the virtode because of noise spread is associated with violation of the coherent structure of the VC.

To analyze the effect of injected electron beam velocity modulation on virtode oscillation characteristics, accelerating voltage (which was the sum of constant quantity U_0 and sinusoidal component $U_0 A\sin(2\pi ft)$, where A is the modulation amplitude

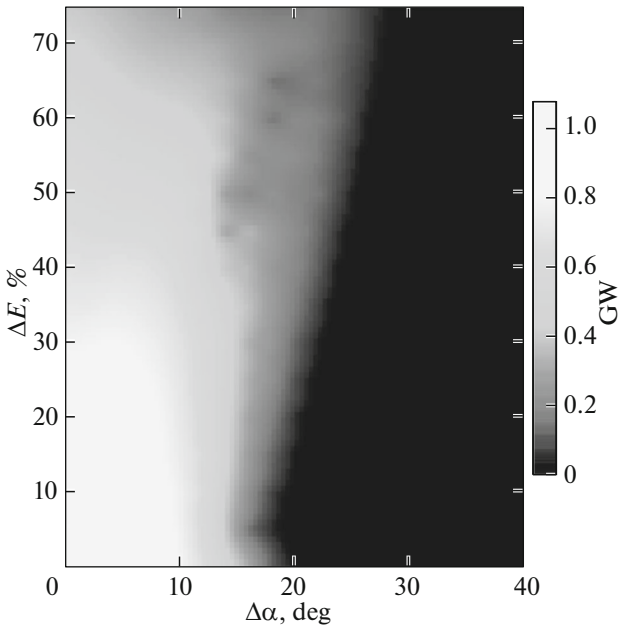

Fig. 3. Dependence of the output signal power of a relativistic virtode with a noise spread of injected electrons on energy spread parameter ΔE and injection angle $\Delta\alpha$. Beam current $I_0 = 9$ kA, $U_0 = 1$ MV.

and f is the modulation frequency) was applied to the anode grid of the gun block of the device. As a result, the electron beam was ejected from the gun block with a modulated velocity.

It was found that the dependence of the integrated output power of the virtode on the modulation frequency is resonant by nature (Fig. 4a): the power attains is maximal value when f coincides with the natural frequency of autonomous virtode oscillation, which is determined by the frequency of the working mode of the first gap of the double-gap cavity. In this way, it is possible to substantially increase the oscillation power and efficiency up to 13%. It should be noted that the additional beam modulation also reduces the duration of the transient process and, accordingly, leads to faster triggering of oscillations. It should be recalled that the signal at the autonomous virtode exit appears after a certain time interval following the transient process, which can be as long as ~100 ns.

The virtode output power is rapidly saturated depending on modulation amplitude A (Fig. 4b), attaining a nearly maximal value for $A \sim 0.05$. Moreover, in the case of equality of f to the natural frequency of the virtode (1.41 GHz in our case), the $P(A)$ dependence (solid curve in Fig. 4b) exhibits a continuous increase changing to saturation. In other cases (e.g., at $f = 1.3$ GHz), the dependence of the output power on the modulation amplitude (dashed curve in Fig. 4b) is more complex and contains a descending segment changing to a further increase. Such a behavior of this dependence can be explained by the nonlinear behavior of the amplitudes of the output signal spectral components, the sum of which determines the output power upon variation of A (Fig. 4c). Indeed, the amplitude of the component at the modulation frequency demonstrates a permanent increase with A, while the amplitude at the natural frequency first increases and then begins to decrease due to the modulation frequency imposed on the beam, which reduces the effectiveness of the beam interaction with the mode excited in the first gap.

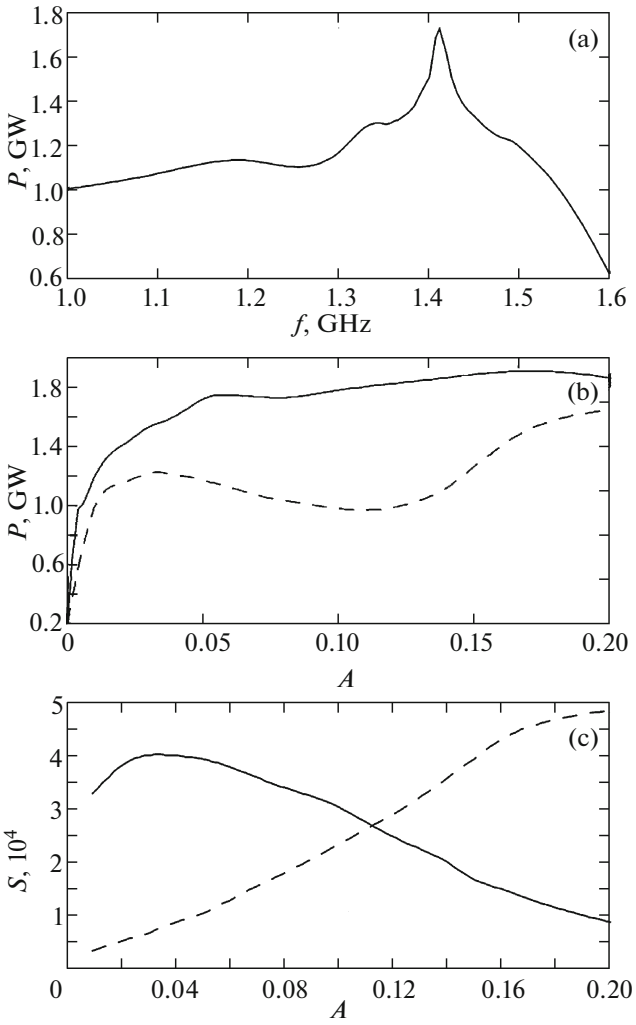

Fig. 4. (a) Dependence of the integrated output power of a relativistic virtode with injected electron beam velocity modulation on modulation frequency f; modulation amplitude $A = 5\%$; (b) dependence of the integrated output power on the modulation amplitude at modulation frequency $f = 1.41$ GHz (solid curve), which is equal to the oscillation frequency of the autonomous virtode, and $f = 1.3$ GHz (dashed curve); (c) dependence of the component amplitudes in the output signal spectrum at the autonomous virtode oscillation frequency $f = 1.41$ GHz (solid curve) and modulation frequency $f = 1.3$ GHz (dashed curve) on modulation amplitude A; modulation frequency $f = 1.3$ GHz; beam current $I_0 = 12.5$ kA, $U_0 = 1$ MV. The time interval over which the integrated output power was estimated is 15–100 ns.

From the physical point of view, the increase in the virtode output power as a result of velocity modulation of the beam at a frequency close to the natural frequency is due to the fact the change in the velocity of new electrons reaching the VC region is in phase with VC natural oscillations, and new (for VC) electrons have "right" velocities, which make it possible to form a denser structure. As a result, the virtode output oscillation power increases.

CONCLUSIONS

We have presented the results of numerical investigation of generation characteristics of the perspective design of a VC oscillator with external feedback (virtode). We have determined the optimal parameters of the system and beam parameters. We have analyzed the effect of beam remodulation in velocity and electron velocity angular spread on virtode generation characteristics. It is shown that the introduction of additional modulation of the electron beam at the natural frequency of the modulation cavity sharply increases the generation efficiency that attains a value of about 13% at the peak. This is due to the effect of resonant interaction of the beam with the electromagnetic field. Additional modulation also reduces the duration of the transient process, which makes it possible to reduce the time of attainment of the working regime. Analysis of the effect of the electron spread in velocity and injection angle have shown that effective generation is possible in a wide range of spreading parameters. This explains low requirements to the beam quality in the virtode. For example, the electron velocity spread up to 30% practically does not affect generation characteristics. Moreover, at large velocity spreads, there is no oscillation failure, although the generation efficiency becomes substantially lower.

Our results lead to the conclusion that oscillators based on a virtual cathode with additional feedback are promising devices for generating superpower microwave radiation. These devices are characterized by a high stability of the oscillation frequency and efficiency for this type of system.

ACKNOWLEDGMENTS

This study was supported by the Ministry of Education and Science of the Russian Federation (project no. 3.859.2017/4.6) and by grant (no. MK-1163.2017.2) for young Russian scientists (candidates of science) from the President of the Russian Federation.

REFERENCES

1. J. Benford, J. A. Swegle, and E. Schamiloglu, *High Power Microwaves* (CRC Press, 2016).
2. R. E. Collin, *Foundations for Microwave Engineering* (Wiley, 2001).
3. R. A. Mahaffey, P. A. Sprangle, J. Golden, et al., Phys. Rev. Lett. **39**, 843 (1977).
4. A. N. Didenko, Ya. E. Krasik, S. F. Perelygin, et al., Pis'ma Zh. Tekh. Fiz. **5**, 321 (1979).
5. D. J. Sullivan, J. E. Walsh, and E. A. Coutsias, in *High Power Microwave Sources*, Ed. by V. Granatstein and I. Alexeff (Artech House, Norwood, 1987), p. 441.
6. *High Power Microwave Sources*, Ed. by V. Granatstein and I. Alexeff (Artech House, Norwood, 1987).
7. S. H. Gold and G. S. Nusinovich, Rev. Sci. Instrum. **68**, 3945 (1997).
8. A. E. Dubinov and V. D. Selemir, J. Commun. Technol. Electron. **47**, 575 (2002).
9. G. Singh and S. Chaturvedi, Phys. Plasmas **18**, 063104 (2011).
10. L. Li, L. Liu, G. Cheng, et al., J. Appl. Phys. **105**, 123301 (2009).
11. L. Li, G. Cheng, L. Zhang, et al., J. Appl. Phys. **109**, 074504 (2011).
12. A. A. Badarin, S. A. Kurkin, A. A. Koronovskii, and A. E. Hramov, Tech. Phys. Lett. **41**, 1148 (2015).
13. A. E. Hramov, S. A. Kurkin, A. A. Koronovskii, et al., Phys. Plasmas **19**, 112101 (2012).
14. J. Ju, D. Cai, G. Du, et al., IEEE Trans. Plasma Sci. **43**, 3522 (2015).
15. A. A. Badarin, S. A. Kurkin, and A. E. Hramov, Bull. Russ. Acad. Sci.: Phys. **79**, 1439 (2015).
16. A. A. Badarin, S. A. Kurkin, A. A. Koronovskii, A. O. Rak, and A. E. Hramov, Plasma Phys. Rep. **43**, 346 (2017).
17. M. V. Fazio, J. Kinross-Wright, B. Haynes, et al., Appl. Phys. **66**, 2675 (1989).
18. A. E. Hramov, A. A. Koronovskii, and S. A. Kurkin, Phys. Lett. A **374**, 3057 (2010).
19. S. A. Kurkin, A. A. Koronovskii, and A. E. Hramov, Tech. Phys. Lett. **37**, 356 (2011).
20. N. S. Phrolov, A. A. Koronovskii, Y. Kalinin, et al., Phys. Lett. A **378**, 2423 (2014).
21. S. C. Burkhart, R. D. Scarpetty, and R. L. Lundberg, J. Appl. Phys. **58**, 28 (1985).
22. R. F. Hoeberling and M. V. Fazio, IEEE Trans. Electromagn. Compat. **34**, 252 (1992).
23. E. B. Abubakirov and A. P. Konyushkov, IEEE Trans. Plasma Sci. **38**, 1285 (2010).
24. N. N. Gadetskii, I. I. Magda, S. I. Naisteter, et al., Plasma Phys. Rep. **19**, 273 (1993).
25. A. S. Shlapakovski, T. Queller, Y. Bliokh, et al., IEEE Trans. Plasma Sci. **40**, 1607 (2012).
26. B. M. Kovalchuk, S. D. Polevin, R. V. Tsygankov, et al., IEEE Trans. Plasma Sci. **38**, 2819 (2010).
27. S. A. Kitsanov, A. I. Klimov, S. D. Korovin, et al., IEEE Trans. Plasma Sci. **30**, 274 (2002).
28. C. K. Birdsall and A. B. Langdon, *Plasma Physics via Computer Simulation* (CRC Press, 2004).
29. S. A. Kitsanov, A. I. Klimov, S. D. Korovin, I. K. Kurkan, I. V. Pegel, and S. D. Polevin, Tech. Phys. **47**, 595 (2002).

Translated by N. Wadhwa